

# Document made available under the Patent Cooperation Treaty (PCT)

International application number: PCT/EP05/001890

International filing date: 23 February 2005 (23.02.2005)

Document type: Certified copy of priority document

Document details: Country/Office: EP  
Number: 04004075.0  
Filing date: 23 February 2004 (23.02.2004)

Date of receipt at the International Bureau: 19 April 2005 (19.04.2005)

Remark: Priority document submitted or transmitted to the International Bureau in compliance with Rule 17.1(a) or (b)



World Intellectual Property Organization (WIPO) - Geneva, Switzerland  
Organisation Mondiale de la Propriété Intellectuelle (OMPI) - Genève, Suisse



**Europäisches  
Patentamt**

**European  
Patent Office**

**Office européen  
des brevets**

*EPOS/1890*

**Bescheinigung**

**Certificate**

**Attestation**

Die angehefteten Unterlagen stimmen mit der ursprünglich eingereichten Fassung der auf dem nächsten Blatt bezeichneten europäischen Patentanmeldung überein.

The attached documents are exact copies of the European patent application described on the following page, as originally filed.

Les documents fixés à cette attestation sont conformes à la version initialement déposée de la demande de brevet européen spécifiée à la page suivante.

**Patentanmeldung Nr.    Patent application No.    Demande de brevet n°**

04004075.0

Der Präsident des Europäischen Patentamts;  
Im Auftrag

For the President of the European Patent Office

Le Président de l'Office européen des brevets  
p.o.

**R C van Dijk**





Anmeldung Nr:  
Application no.: 04004075.0  
Demande no:

Anmeldetag:  
Date of filing: 23.02.04  
Date de dépôt:

Anmelder/Applicant(s)/Demandeur(s):

Schott Spezialglas GmbH  
Hattenbergstrasse 10  
55122 Mainz  
ALLEMAGNE

Bezeichnung der Erfindung/Title of the invention/Titre de l'invention:  
(Falls die Bezeichnung der Erfindung nicht angegeben ist, siehe Beschreibung.  
If no title is shown please refer to the description.  
Si aucun titre n'est indiqué se référer à la description.)

Process for preparing CaF<sub>2</sub> lens blanks especially for 193 nm and 157 nm  
lithography with minimized defects

In Anspruch genommene Priorität(en) / Priority(ies) claimed /Priorité(s)  
revendiquée(s)

Staat/Tag/Aktenzeichen/State/Date/File no./Pays/Date/Numéro de dépôt:

Internationale Patentklassifikation/International Patent Classification/  
Classification internationale des brevets:

C03B/

Am Anmeldetag benannte Vertragsstaaten/Contracting states designated at date of  
filing/Etats contractants désignées lors du dépôt:

AT BE BG CH CY CZ DE DK EE ES FI FR GB GR HU IE IT LU MC NL  
PT RO SE SI SK TR LI

Bemerkungen:

Remarks:

Remarques:

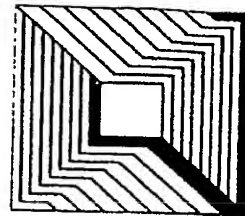
The application was transferred from the above mentioned original applicant to:  
SCHOTT AG - Mainz/DE  
The registration of the changes has taken effect on 09.10.2004



PATENTANWÄLTE  
**FUCHS MEHLER WEISS & FRITZSCHE**  
WIESBADEN – MÜNCHEN – ALICANTE

EPO - Munich  
37

23. Feb. 2004



European Patent Attorneys  
European Trademark Attorneys

**Büro/Office München**

Dr. Thomas M. Fritzsche  
Dipl.-Chem. und Biologe

Naupliastraße 110  
D-81545 München

Telefon: 089/5 23 17 09  
Telefax: 089/52 24 05  
e-mail: fuchs-pat@t-online.de

P 2395/sg

Dr. Ing. Jürgen H. Fuchs  
Dipl.-Ing., B. Com.  
Dr. rer.nat. Klaus Mehler  
Dipl.-Phys.  
Dipl.-Ing. Christian Weiß  
Dipl.-Ing. Kurt Müller

Dipl.-Phys. Werner Witzel  
Abraham-Lincoln-Straße 7  
D-65189 Wiesbaden

Postfach 46 60  
D-65036 Wiesbaden  
Telefon: 0611/71 42-0  
Telefax: 0611/71 42-20  
e-mail: fuchs-pat@t-online.de

Paseo Explanada de  
España No. 3. 5-dcha  
ES-03002 Alicante  
Telefon: +34/96/5 20 01 34  
Telefax: +34/96/5 20 02 48

---

**Process for preparing  $\text{CaF}_2$  lens blanks especially for  
193 nm and 157 nm lithography with minimized defects**

---

Schott Spezialglas GmbH  
Hattenbergstrasse 10  
55122 Mainz  
DE

Ust.-ID-Nr./VAT REG No.  
DE 113895983

Postbank München  
Konto 2403 67-806  
(BLZ 700 100 80)

Volksbank Freudenstadt  
Konto 268 360 09  
(BLZ 642 910 10)

23. Feb. 2004

Schott Spezialglas GmbH

P 2395/PI

Process for preparing  $\text{CaF}_2$  lens blanks especially for  
193 nm and 157 nm lithography with minimized defects

The invention relates to a process for critical parameters  
of  $\text{CaF}_2$  lens blanks for 193 nm and 157 nm lithography.

Homogeneity residuals of the refractive index have a strong  
influence on the performance of lithography tools for both  
193 and 157 nm application wavelengths. By systematic  
investigations of various defects in the real structure of  
 $\text{CaF}_2$  crystals, the origin of homogeneity residuals can be  
shown. Based on a quantitative analysis we define limiting  
values for the individual defects which can be either  
tolerated or controlled by optimized process steps, e.g.  
annealing. These correlations were carried out for all  
three relevant main crystal lattice orientations of  $\text{CaF}_2$   
blanks. In conclusion we achieved a strong improvement of  
the critical parameters of both refractive index  
homogeneity and striae for large size lens blanks up to  
270mm diameter.

The trend towards ever smaller structures in semiconductor  
devices is still driven by Moores Law. A major part in the  
production process for semiconductor devices is optical  
lithography. The optics used in these lithography tools  
require materials of exceptional high quality. Due to the

application wavelength of 193nm or in the future 157nm  $\text{CaF}_2$  single crystalline lenses are a major part in the optics of this systems. Among other parameters the refractive index homogeneity has a strong influence on the image quality.

G. Grabosch, K. Knapp, E. Moersen: "Status of the  $\text{CaF}_2$  Program at Schott Lithotec", 2<sup>nd</sup> International Sematech 157nm Technical Data Review Meeting, May 2002; G. Grabosch, K. Knapp, L. Parthier, Th. Westerhoff, E. Moersen: "Calcium Fluoride Quality Improvements Support Availability of First  $\text{F}_2$  Lithography Tools", 3<sup>rd</sup> International Sematech 157nm Technical Data Review Meeting, Sep. 2002; and J. Hahn, G. Grabosch, L. Parthier, K. Knapp: "Quality Status for 157nm Exposure Tools", International Sematech & Selete 4<sup>th</sup> International Symposium on 157nm Lithography, Aug. 2003 describe that during the production of  $\text{CaF}_2$  single crystals several process steps will influence the optical property of the material. In order to further optimize the material various defects occurring due to real structure, their influence on optical homogeneity and a method of controlling them during processing were now investigated by the present inventors.

The parameters in homogeneity of the refractive index and stress-induced birefringence (SDB) must also be very low for lenses having large diameters. Thereby these parameters should preferably show an inhomogeneity (after subtraction of 36 Zernike coefficients) of lower than 0.02 ppm and the SDB-(RMS) should preferably be less than 0.2 nm/cm in the (111) direction, in the (100) direction it should be less



than 0.4 nm/cm. According to the invention, this can be obtained by an optimized tempering in a separate temperature furnace which preferably is optimally constructed.

These quality parameters are now not anymore determined by global, i. e. wide-ranging defects in crystal structures and characteristics but are rather determined by local inhomogeneities. These local inhomogeneities are based on different local defects in the theoretically completely periodical crystal structure. In the present invention the influence of each single defect has been investigated on local effects, e.g. as optical inhomogeneity before and after tempering. The influence of tempering has been investigated for each main orientation (111, 100, 110) on  $\text{CaF}_2$  blanks. The invention now enables to determine limits for each structural defect and each main orientation before the tempering, thus making it possible to achieve aimed parameters by an adopted, e.g. high temperature, tempering.

The most common crystal defects affecting the refractive index homogeneity in  $\text{CaF}_2$  are slip planes and small angle grain boundaries and other local real structure defects.

The main method of plastic deformation of crystals is glide. During gliding one part of the crystal is displaced relative to another. Glide occurs over definite crystallographic planes along definite directions. The planes along which the crystal layers move are the slip planes and the direction of the displacement is the slip

direction. On a microscopic scale the glide process can be explained with the movement of dislocations through the crystal. A set of all crystallographically equivalent slip planes and directions forms a glide system. For  $\text{CaF}_2$  the principle glide system is  $\{100\}/\langle 110 \rangle$ . Further slip plane systems are  $\{110\} / \langle 110 \rangle$  and at higher temperatures  $\{111\} / \langle 110 \rangle$  (see L. A. Shuvalov ed.: "Modern Crystallography IV" Springer Series in Solid State Sciences 37, pp. 77).

Small angle grain boundaries are two dimensional lattice defects comprised of a number of step and / or screw dislocations. They are confined to small volumes. Depending on the misorientation angle, the inclination of the grain boundary and the translational displacement between neighboring sub grains, two types of sub grain boundaries can be distinguished: tilt and twist boundaries. One refers to small angle grain boundaries in case the difference in orientation is small, i.e. in the range of minutes up to a few degrees. Small angle grain boundaries can be formed e. g. during crystal growth caused by thermal fluctuations at the solid liquid interface and or impurities at the interface. Normally small angle grain boundaries are accompanied by a short range stress field.

In some cases small angle grain boundaries rearrange and form more extended structures. These structures are not aligned to a specific crystallographic direction and occur as a local distortion in the homogeneity interferograms. These distortions have also a detrimental effect on the optical image quality.

Fig. 1 shows the influence of Zernike terms subtracted on PV (Peak to Valley, which is the maximal difference between the highest and lowest value measured within a blank.) and RMS.

In the framework of our ongoing process of quality improvement we investigated the influence of the annealing process on the homogeneity in (100), (110) and (111) oriented  $\text{CaF}_2$  lens blanks. Therefore homogeneity wave fronts were taken under the same conditions before and after annealing. The interferometer used is a ZEISS D100 Fizeau type interferometer, the spatial resolution was  $0.2 \mu\text{m}$ . Before analyzing the wave fronts for crystal defects 36 Zernike terms were subtracted. In this residual wave front crystal defects can be detected and analyzed more easily. A subtraction of further Zernike terms did not improve the results due to an asymptotic effect on PV and RMS as shown in Figure 1.

Fig. 2 shows an example of performed fitting of a defect structure cross section before annealing (thin line), and after annealing (bold line).

The analysis performed as follows:

Before and after annealing the strongest defect structures in the wave front was analyzed. Then for the individual defect structures a Gaussian fit of the cross sections were performed. The fit provide values for amplitude and half width. The observed change in amplitude and half width due

to annealing of corresponding defect structures are calculated relative to the starting value.

Fig. 3 shows a cross section scan in homogeneity wave front before (Fig. 3a) and after annealing (Fig. 3b) of a crystal.

For a better illustration of the applied procedure in the following the analysis considering as example a blank with untypical high defect level (Figure 3 a, b) will be discussed. Homogeneity wave fronts after subtraction of 36 Zernike terms before and after annealing is compared. After annealing an improvement of the total residual structure can clearly be seen. Whereas before annealing the homogeneity is dominated by long range structures, after annealing homogeneity is more affected by the short range defect structures. The relative improvement of RMS-Residual is about 30%. While the maximum amplitude of a single local structure defect could be reduced to 60% of the starting value the corresponding maximum half width could be minimized down to 30%.

Each defect structure observed is categorized for type and blank orientation. For the values found typical for the defect behavior the mean value was calculated. The results obtained are discussed below.

The annealing process has only a very small influence on small angle grain boundaries in  $\{111\}$  oriented lens blanks. The reduction of the amplitude was in the range of about

20%, the width was nearly constant. For other orientations a similar behavior can be achieved.

In a modified form small angle grain boundaries generate more extended defect structures. In spite of the "normal" small angle grain boundary we find a clear orientation dependence for the annealing performance. While we obtained a 20 % reduction for the amplitude and about 30% for the half width for {100} and {110} orientation, whereas the values for {111} a mostly unchanged.

During the annealing process slip planes become activated and relax along glide systems. For CaF<sub>2</sub> this is in general the {100} / <110> glide system. In case small angle grain boundaries are present they can hamper the relaxation of the slip planes.

The annealing results show a strong improvement for all blank orientations. Especially for the {111} orientation the slip planes can completely disappear. That means slip planes are not dominating the residual of the refractive index homogeneity. For the other orientations the amplitude can be reduced by a factor up to 5.

From the results discussed above it is now for the first time possible to define critical maximum values for the different real structure phenomena before annealing for each orientation. Under these conditions the annealed lens blanks reach the required quality for the residual homogeneity.

The invention has therefore for its aim to provide a classification method according to which it is possible to classify defects in a crystal structure e.g. as slip planes, small angle grain boundaries, linear structures and others, as well as mixed structural defects. According to the invention, an image of a homogeneity (e.g. as shown in Fig 3) is established (preferably with a CCD-Camera) a single structure (defect) is analysed by measuring homogeneity in said image and determining the RMS-value (36 Zernike coefficients subtracted) for said structure or defect. Thereby, a line scan is obtained from the structure and the local defect is identified as a peak. This peak is defined by a Gaussian fit with the parameters height of the peak (amplitude) and half-width. Both are found to be absolute values for the blank as shown in Fig. 2. By integrating the length of said defect in said homogeneity image, the amount of the defect can be calculated from the overall value of the blank. Thereby, the influence of each single defect on the overall value becomes determinable. The above analysis is done before and after the tempering of the blank. On the basis of this analysis, an evaluation of the influence of each defect structure and defect type in each single blank on each critical parameter becomes possible.

According to the invention, it is now possible to effectively determine these blanks for which a tempering is possible and limiting values can be defined.

In the following we present achieved improvements for the most difficult {100} oriented lens blanks.

Through a better approach for describing the blank quality as described above it is now possible to improve the material quality of our  $\text{CaF}_2$  lens blank material. The following Table 1 shows the average and standard deviation values achieved for (100) oriented lens blanks for two main quality parameters. The introduction of the advanced conditions lead to a 31% decrease of the stress birefringence RMS value. For the refractive index homogeneity a similar large quality enhancement of about 26% could be realized. Especially the reduction of the short range refractive index homogeneity is of considerably importance since this parameter causes flare in the imaging.

The reproducibility as represented by the standard deviation in line 2 is essential for the production process. For both parameters we achieve a significant progress. For stress birefringence the new conditions lead to reduction of the scattering of the values by a factor of 2. The advancement for homogeneity is even larger. The reduction is of a factor of approx 5.

The quality level of these (100) oriented lens blanks meets the currently known requirements for the application in projection optics for both 193nm and 157nm wavelength.

The following Table 1 shows the achieved quality improvement for stress birefringence and short range

refractive index homogeneity for (100) oriented  $\text{CaF}_2$ -crystals:

New conditions		Old conditions	
SBR(rms) average [nm/cm]	Short range refractive index homogeneity, average	SBR(rms) average [nm/cm]	Short range refractive index homogeneity average set =1
0,37	0,74	0,54	1
$\pm 0,08$	$\pm 0,09$	$\pm 0,16$	$\pm 0,44$

Table 1

Fig. 4 shows the short range refractive index homogeneity for (100) oriented  $\text{CaF}_2$  lens blank before (Fig. 4a) and after improvement (Fig. 4b).

Figures 4a and 4b illustrate the reduction of local defect structures as reflected by the short range refractive index homogeneity for champion lens blanks. Figure 4a clearly shows the residual of defect structures after annealing. The remaining structures are mainly slip planes but also small angle grain boundaries in different modifications are visible. Through the measures applied the remaining crystal defects could be reduced to a very low level. Figure 4b shows that the primary slip plane system  $\{100\} / \langle 110 \rangle$  has



disappeared and only a few traces indicate the secondary system running along  $\{111\}$  /  $\langle 110 \rangle$ . No other defect structures can be observed.

The influence of various crystal defects on the optical material quality of  $\text{CaF}_2$  is determined. With the process of the invention including further improvement of the annealing process applied to critical (100) oriented  $\text{CaF}_2$  lens blanks the amount of defect structures can be reduced significantly.

\*\*\*

23. Feb. 2004

## Claims

1. Process for classifying structural defects in a crystal structure, characterized in that an homogeneity image showing simple structures of a crystal blank is established and said single structure is analysed by measuring the homogeneity of RMS-value of said single structure, defining a peak by a Gaussian fit with peak amplitudes and half-width and integrating the length of this single structure in a homogeneity image.

2. Process according to claim 1, characterized in that the ratio of said integrated value of said defect and the overall value of the blank is determined, thereby characterizing the influence of a single defect on the overall homogeneity of said blank.

\*\*\*



## Abstract

Process for critical parameters of  $\text{CaF}_2$  lens blanks for  
193 nm and 157 nm lithography

Homogeneity residuals of the refractive index have a strong influence on the performance of lithography tools for both 193 and 157 nm application wavelengths. By systematic investigations of various defects in the real structure of  $\text{CaF}_2$  crystals, the origin of homogeneity residuals can be shown. Based on a quantitative analysis we define limiting values for the individual defects which can be either tolerated or controlled by optimized process steps, e.g. annealing. These correlations were carried out for all three relevant main crystal lattice orientations of  $\text{CaF}_2$  blanks. In conclusion we achieved a strong improvement of the critical parameters of both refractive index homogeneity and striae for large size lens blanks up to 270mm diameter.



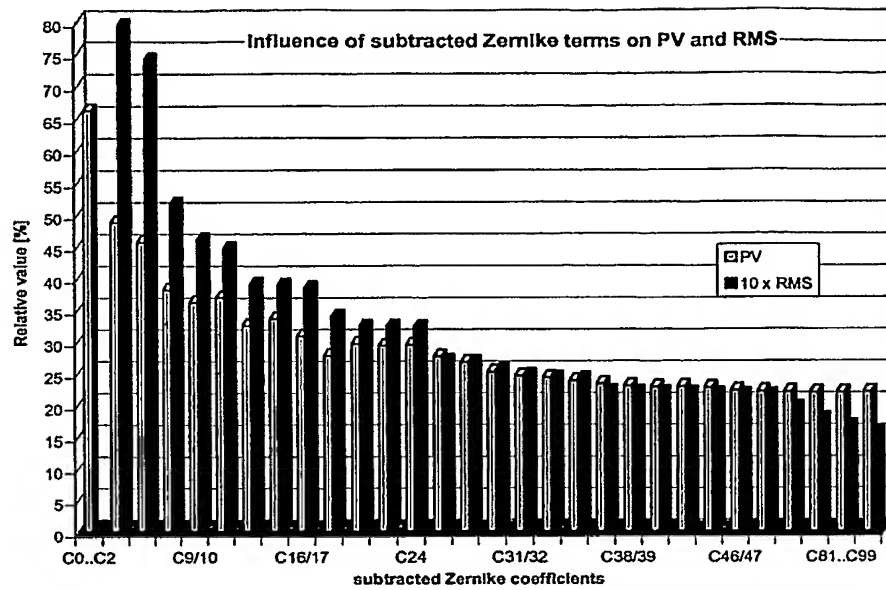


Fig.1.

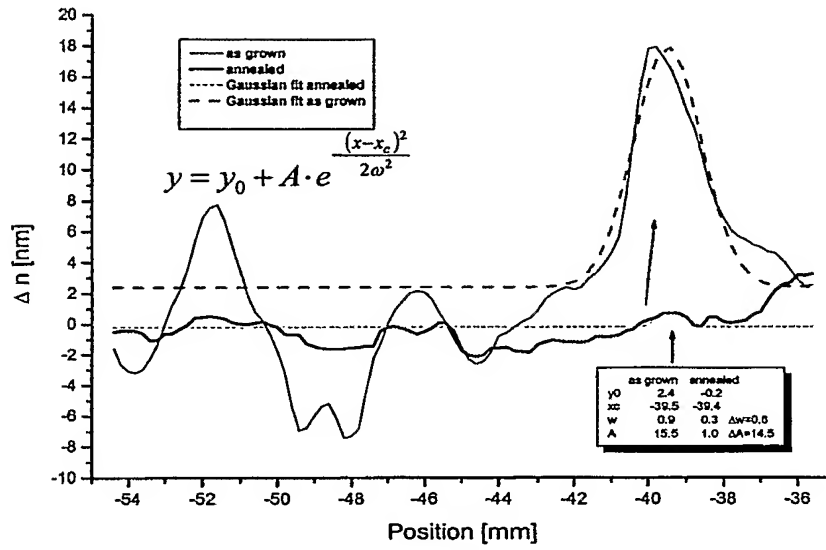


Fig. 2:

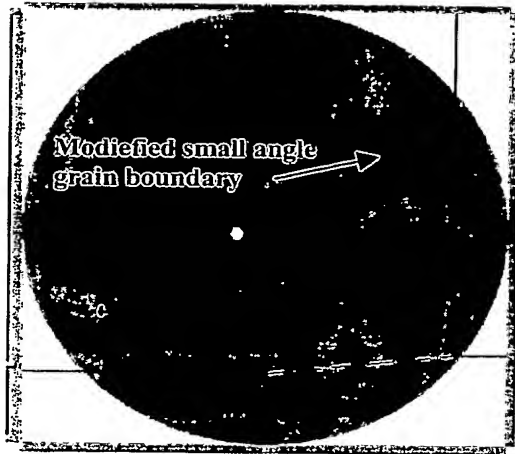


Fig. 3a.

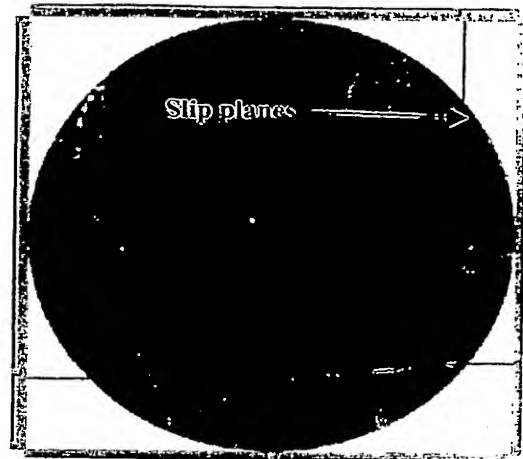
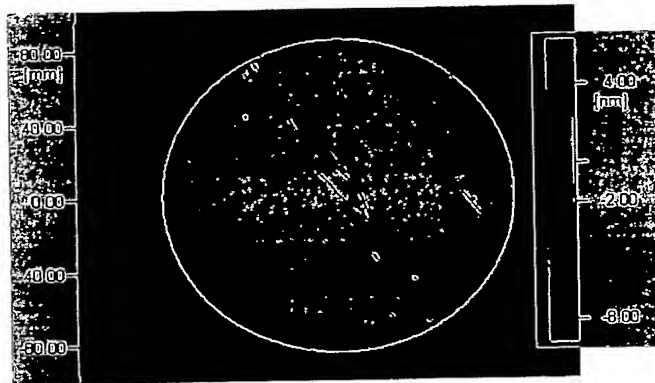


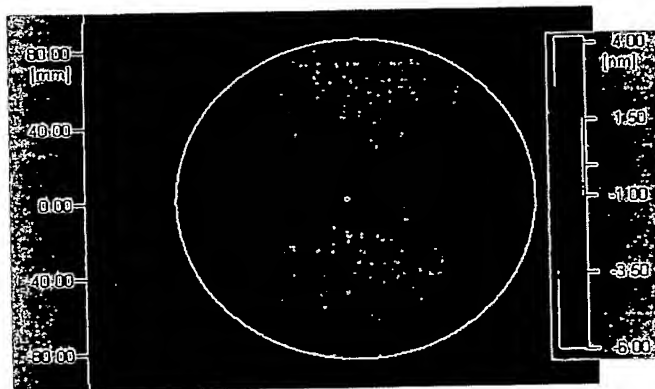
Fig 3b.





a. u.  
Fig. 4a:

1



a. u.  
Fig. 4b:

0.38